Phase-dispersion optical tomography

Changhuei Yang, Adam Wax, Ramachandra R. Dasari, and Michael S. Feld

George Harrison Spectroscopy Laboratory, Massachusetts Institute of Technology, Cambridge, Massachusetts 02139

Received October 25, 2000

We report on phase-dispersion optical tomography, a new imaging technique based on phase measurements using low-coherence interferometry. The technique simultaneously probes the target with fundamental and second-harmonic light and interferometrically measures the relative phase shift of the backscattered light fields. This phase change can arise either from reflection at an interface within a sample or from bulk refraction. We show that this highly sensitive (~5°) phase technique can complement optical coherence tomography, which measures electric field amplitude, by revealing otherwise undetectable dispersive variations in the sample. © 2001 Optical Society of America

OCIS codes: 050.5080, 110.4500, 180.3170, 240.6700.

We recently developed a robust and highly sensitive imaging technique, phase-dispersion microscopy, that uses low-coherence interferometry to measure the optical phase of light transmitted through a thin sample.[1] The key idea is the use of a pair of harmonically related low-coherence light sources to eliminate motional artifacts in the interferometer and the target, which usually prevent accurate measurements of phase information. As with phase contrast microscopy, one can use this technique to study unstained tissue sections by rendering subtle refractive-index differences visible. Phase-dispersion microscopy is related to optical coherence tomography (OCT),[2] a valuable technique for imaging *in vivo* biological tissues, as both are based on low-coherence interferometry. OCT provides information about the scattering properties of subsurface structures through measurement of the amplitude of the backscattered electric field. It was recently demonstrated that interferometric methods that measure phase information can provide additional information about the birefringence,[3] dispersion,[1] and spatial phase variation[4] of a sample.

In this Letter we report a tomographic implementation of phase-dispersion microscopy. This technique, which we call phase-dispersion optical tomography (PDOT), combines the ability of phase contrast microscopy to image transparent objects with the capability of OCT to obtain depth-resolved images. We demonstrate that this method can extract quantitative dispersion information about embedded structures. In addition, we show that PDOT can measure the intrinsic phase shift that is due to reflection at an interface. Finally, we show that PDOT can reveal dispersion-based differences that are not detectable with OCT.

PDOT employs a modified OCT system, based on the Michelson interferometer arrangement shown in Fig. 1. The input light is a two-color composite beam composed of fundamental and second-harmonic laser light. The light source is a low-coherence Ti:sapphire laser producing 150-fs pulses at 816 nm with a beam diameter of 2.1 mm (FWHM) at the input to the interferometer. The second harmonic at 408 nm, with a beam diameter of 1.1 mm (FWHM), is generated by a standard frequency doubler. The composite beam is divided in two at the beam splitter. One part (the signal) is brought to a focus in the target sample, while the other (the reference) is focused on a stationary reference mirror. Maintaining the focal spots in the signal and the reference arms at the same distance from the beam splitter ensures optimal interference. The powers of the 408- and 816-nm beam components at the sample are 7.0 and 2.8 mW, respectively. Achromatic 10× microscope objectives focus the composite beam onto the sample with a FWHM of ~7 μm at both wavelengths. The sample, which is mounted on a translation stage, is axially scanned at a constant velocity of 1 mm/s. The motion serves two functions: It confers a Doppler shift upon the reflected beam, and it translates the focal spot through the sample. A second translation stage moves the sample laterally between each axial scan. The backreflected beams are recombined at the beam splitter, separated by their wavelength components by use of a dichroic mirror, and measured separately by photodetectors. The resulting heterodyne signals at both wavelengths are measured and digitized by a 16-bit 100-kHz analog–digital converter. The signals are bandpassed around their center heterodyne frequencies and Hilbert transformed, allowing us to extract their corresponding phases, Ψ_1 and Ψ_2.[5,6] (The subscripts 1 and 2 denote the fundamental

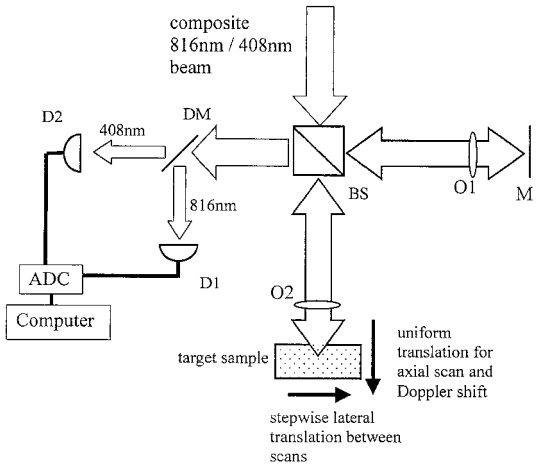

Fig. 1. Experimental setup: M, reference mirror; BS, beam splitter; O1, O2, microscope objectives; D1, D2, photodetectors; DM, 408-nm/816-nm dichroic mirror. ADC, analog-to-digital converter.

0146-9592/01/100686-03$15.00/0

and the second-harmonic wavelength components, respectively.)

It can be seen that jitter of magnitude Δx in either the signal or the reference-arm length will vary phases Ψ_1 and Ψ_2 by $k_1\Delta x$ and $k_2\Delta x$, respectively, where k_1 and k_2 are the free-space wave numbers. As k_2 is exactly double k_1, we can totally eliminate the effect of this jitter by subtracting twice Ψ_1 from Ψ_2.[1,7] The resulting phase difference, $\Psi_R(L)$, can be expressed in terms of the sample's properties:

$$\Psi_R(L) = \mathrm{mod}_{2\pi}\left\{2k_1\int_0^L [n_1(z) - n_2(z)]\mathrm{d}z + 2\phi_1 - \phi_2\right\}, \tag{1}$$

where z is the axial direction, L is the depth of the focal spot in the sample, $n_1(z)$ and $n_2(z)$ are the spatially varying refractive indices of the sample, and ϕ_1 and ϕ_2 are the phase shifts that are due to the interface at the focal spot. We measure $\Psi_R(L)$ with a sensitivity of 9×10^{-2} rad.[7]

When the uppermost surface of the sample is probed ($L = 0$), $\Psi_R(L)$ reduces to

$$\Psi_R(L = 0) = \Psi_{\mathrm{interface}} = \mathrm{mod}_{2\pi}(2\phi_1 - \phi_2). \tag{2}$$

We note that, unlike phase-based techniques, which measure the phase difference between two adjacent points,[4,8] our technique provides intrinsic phase information, in the form of $\Psi_{\mathrm{interface}}$, at the point that is probed.

The ability to measure $\Psi_{\mathrm{interface}}$ can be used to characterize interfaces. The phase shift associated with reflection from a higher-index dielectric surface is exactly 180°, independent of wavelength. Reflection from more complicated surfaces, such as metals, can exhibit a wavelength-dependent phase shift. As demonstrated by Matsumoto,[9] metallic surfaces can have nontrivial phase shifts. In addition, coatings deposited on optical mirrors can also exhibit spectrally dependent phase shifts. Lastly, the packing arrangement and the particulate size of complex surfaces, such as those of an opal diffuser, can cause wavelength-dependent phase shifts.

As a demonstration of PDOT's ability to acquire phase-shift information, we measured $\Psi_{\mathrm{interface}}$ for several surfaces: dielectrics, coated mirrors, an opal diffuser, and gold. The results are presented in Table 1. A glass slide was used for calibration, as it is a dielectric material, and thus $\Psi_{\mathrm{interface}}$ is 180°. The second dielectric sample, a magnesium fluoride slide, gave $\Psi_{\mathrm{interface}} = (179.8 \pm 0.7)°$, demonstrating the accuracy of the technique. In addition, the measured $\Psi_{\mathrm{interface}}$ from a gold coin is in good agreement with published values for electroplated gold.[10] Finally, we verified experimentally that the values of $\Psi_{\mathrm{interface}}$ associated with an opal diffuser and with different types of mirror coatings are distinctly different.

As PDOT can provide depth resolution, it can also be applied to multiple-layer targets to reveal dispersion information about each layer. The target, shown in Fig. 2(a), consists of side-by-side 90-μm-thick segments of water and 20% volume-concentration gelatin, sandwiched between 170-μm-thick microscope coverslips. The arrangement rests upon a flat Newport AL.2 mirror. The PDOT phase image of the sample is shown in Fig. 2(b). For clarity, $\Psi_R(L)$ is plotted for a given interface for the region at which the heterodyne signal is more than half of the maximum signal associated with that interface. The light reflected from the first glass-gelatin/water interface gives rise to a phase difference, $\Psi_R(L)$, that is uniform across the lateral scan. This constant phase difference is as predicted by Eq. (1), where the uniformity of the microscope coverslip implies that $\int_0^L [n_1(z) - n_2(z)]\mathrm{d}z$ is constant, and the lower refractive indices of both water and the gelatin relative to the coverslip ensure that ϕ_1 and ϕ_2 are zero. The light reflected from the top and bottom surfaces of the second glass coverslip has traversed either gelatin or water. Thus, $\Psi_R(L)$ varies across the lateral scan.

Since all interfaces in the sample are well characterized as either dielectric–dielectric or dielectric–mirror, we know all ϕ_1 and ϕ_2 values. By substituting the phase shifts into Eq. (1) and subtracting $\Psi_R(L)$ of the interfaces associated with a given layer, we can extract the phase shift between the 408- and the 816-nm light for each layer, because of refractive-index differences between the two wavelengths. This intrinsic dispersive phase shift, $\Psi_{D,i}(L_i)$, for the ith layer can be expressed as

$$\Psi_{D,i}(L_i) = \mathrm{mod}_{2\pi}[2k_1(n_{1,i} - n_{2,i})L_i], \tag{3}$$

where L_i is the thickness of the layer. Figure 2(c) shows a false-color image of the sample based on $\Psi_{D,i}(L_i)$. The regions of gelatin and water are clearly distinct, and the bottom coverslip now appears uniform. In addition, by comparing $\Psi_{D,i}(L_i)$ of water and gelatin, we can quantitatively evaluate the difference between $(n_1 - n_2)$ for water and $(n_1 - n_2)$ for gelatin as $(3.07 \pm 0.05) \times 10^{-3}$. We note that $\Psi_{D,i}(L_i)$ is inherently limited to modulus 2π. Therefore, should the difference be large enough that $\Psi_{D,i}(L_i)$ wraps over as we scan across the two regions, the step size used should be sufficiently fine that this phase wrapping can be tracked.

Table 1. Measurements of $\Psi_{\mathrm{interface}}$ for Various Surfaces

Sample	$\Psi_{\mathrm{interface}}$	$\Psi_{\mathrm{interface}}$ (Theory)
Microscope glass slide	$(180.0 \pm 1.6)°$	180° (calibration set)
MgF_2 slide	$(179.8 \pm 0.7)°$	180° (dielectric)
Newport mirror		
AL.1	$(344.8 \pm 0.6)°$	
AL.2	$(232.6 \pm 1.2)°$	
ER.1	$(336.8 \pm 1.4)°$	
ER.2	$(235.4 \pm 0.5)°$	
BD.2	$(67.6 \pm 1.4)°$	
Edmund Scientific opal diffuser	$(182.4 \pm 0.7)°$	
Gold (99.9% purity coin)	$(176.1 \pm 2.4)°$	173° (for electroplated gold)

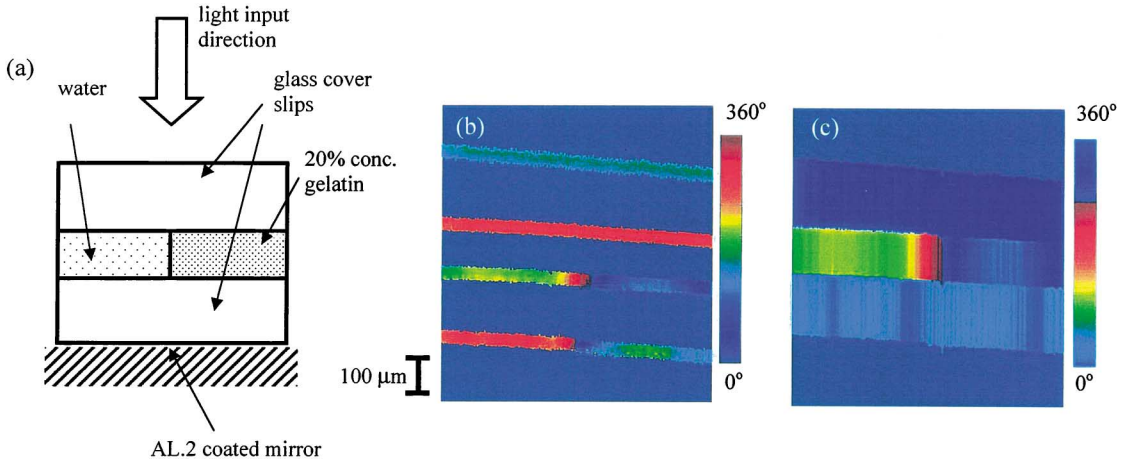

Fig. 2. Images of the sample studied with PDOT: (a) geometrical arrangement; (b) PDOT phase image, $\Psi_R(L)$; (c) processed PDOT image, in which the intrinsic dispersion-related phase shift, $\Psi_{\mathrm{Di}}(L_i)$, is plotted.

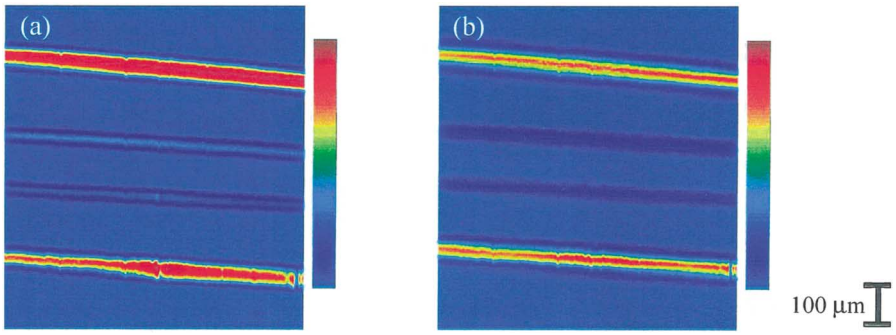

Fig. 3. OCT images of the sample: (a) 816 nm, (b) 408 nm.

For comparison, Figs. 3(a) and 3(b) show the corresponding OCT images of the samples at 816 and 408 nm. As can be seen, the amplitude-based approach is unable to detect any difference between the gelatin and water regions. PDOT can thus complement OCT by providing additional phase information about the target.

In this Letter we have demonstrated that PDOT is a practical and robust method of extracting depth-resolved phase information. We showed that this information is quantitative and reveals the phase shift that is due to reflection at an interface and (or) dispersion of a bulk material, even when the target region is below the surface. The technique can provide a highly sensitive noncontact means of verifying the quality of materials in fabrication processes. Moreover, as demonstrated in a recent paper on phase-dispersion microscopy,[1] this phase-based technique is very sensitive to small differences in biological samples that manifest themselves as wavelength-dependent changes in the index of refraction. Since the technique eliminates motional artifacts, it is well suited for performing phase-based measurements of *in vivo* tissues and thus has potentially important clinical applications.

This work was carried out at the Laser Biomedical Research Center of the Massachusetts Institute of Technology and was supported by National Institutes of Health (NIH) grant P41-RR02594, National Science Foundation grant 9708265-CHE, and a grant from Hamamatsu Corporation. A. Wax was supported by NIH National Research Service Award 1 F32 RR05075-01. We acknowledge helpful comments about the mirrors from Anna Wang and Earl Rudisill of Newport Corporation. C. Yang's e-mail address is chyang@mit.edu.

References

1. C. Yang, A. Wax, I. Georgakoudi, E. B. Hanlon, K. Badizadegan, R. R. Dasari, and M. S. Feld, Opt. Lett. **25,** 1526 (2000).
2. J. A. Izatt, M. R. Hee, D. Huang, E. A. Swanson, C. P. Lin, J. S. Schuman, C. A. Puliafito, and J. G. Fujimoto, Opt. Photon. News **4**(10) 14 (1993).
3. J. F. de Boer, T. E. Milner, M. J. C. van Gemert, and J. S. Nelson, Opt. Lett. **22,** 934 (1997).
4. C. K. Hitzenberger and A. F. Fercher, Opt. Lett. **24,** 622 (1999).
5. Y. Zhao, Z. Chen, C. Saxer, S. Xiang, J. F. de Boer, and J. S. Nelson, Opt. Lett. **25,** 114 (2000).
6. A. B. Carlson, *Communication Systems*, 3rd ed. (McGraw-Hill, New York, 1986).
7. C. Yang, A. Wax, and M. S. Feld, Opt. Lett. **26,** 235 (2001).
8. E. Cuche, F. Bevilacqua, and C. Depeursinge, Opt. Lett. **24,** 291 (1999).
9. H. Matsumoto, Rev. Sci. Instrum. **65,** 2894 (1994).
10. R. C. Weast, ed., *CRC Handbook of Chemistry and Physics*, 64th ed. (CRC, Boca Raton, Fla., 1983).